

## Research Article

# Physicochemical and Rheological Characterization of a Novel Manna Exudate from *Alhagi pseudalhagi* (Iranian Tarangabin)

Shahriyar Salehi <sup>1</sup>, Fatemeh Raouf Fard <sup>2</sup>, Seyed Mohammad Hashem Hosseini <sup>1</sup>, Hadi Hashemi <sup>1</sup>, and Mehrdad Niakousari <sup>1</sup>

<sup>1</sup>Department of Food Science and Technology, School of Agriculture, Shiraz University, Shiraz, Iran

<sup>2</sup>Department of Horticultural Sciences, School of Agriculture, Shiraz University, Shiraz, Iran

Correspondence should be addressed to Mehrdad Niakousari; mehrnia2012@yahoo.com

Received 5 June 2023; Revised 6 April 2024; Accepted 2 May 2024; Published 20 May 2024

Academic Editor: Maria Concetta Strano

Copyright © 2024 Shahriyar Salehi et al. This is an open access article distributed under the Creative Commons Attribution License, which permits unrestricted use, distribution, and reproduction in any medium, provided the original work is properly cited.

Tarangabin manna (TM) is a resinous substance having a yellowish sticky character with a reasonably sweet taste. It is largely collected in Iran and Afghanistan. This study for the first time presents a comprehensive investigation of the techno-functional, rheological, and interfacial characteristics of water-soluble components for TM. The composition analysis revealed protein, moisture, fat, ash, and carbohydrate contents of 1.58, 2.98, 0.51, 2.04, and 92.90%, respectively. The effects of TM concentration on the physicochemical, structural, rheological, interfacial, emulsion, and foaming ability and stability were evaluated. X-ray diffraction analysis showed an amorphous structure for the purified sample and a crystalline structure for the raw sample. TM solutions exhibited Newtonian behavior, with the apparent viscosity decreasing as temperature increased, fitting well with the Arrhenius model. The TM solutions exhibited weak viscoelastic properties, primarily demonstrating a dominant viscous character. The surface tension and interfacial tension of the TM solution prepared at a concentration of 50% were measured at 45.23 mN/m and 7.74 mN/m, respectively. The contact angle of the dry thin layer of TM was determined to be 31.74°. Remarkably, the TM solution at a concentration of 50% exhibited the highest foaming ability (76.80%), foaming stability (91.92%), and emulsifying activity index (24.53%). The findings, coupled with TM appropriate foaming ability and stability, sweetness, and characteristic flavor, suggest that TM holds potential as a special food ingredient.

## 1. Introduction

Tarangabin manna (TM) is sweet, yellowish in color and semiliquid exudate, created on the aerial parts of some *Alhagi* genera, such as *Alhagi pseudalhagi* or *Alhagi maurorum* (Camelthorn). It is produced by an insect called *Poophilus nebulosus* Leth. (belongs to the genus *Larinus*, *Cercopidae* family, *Homoptera* phylum), which lives on the aerial parts of the plant. To be precise, TM is the exudation of this insect produced after nourishment on the plant, which crystallizes and dries on the plant. It should be pointed out that TM is not producible from all genera of *Alhagi*, while the climate condition also plays an important role in its formation. Special attention has been paid to TM in some major *Materia Medica* manuscripts of the Islamic era as one

of the most commonly used medicinal matters in Islamic Traditional Medicine. In Greek medicine, “manna” is a collective term used to describe the extraction of sweet resin from the leaves and stems of the plant. *A. maurorum*, growing naturally in the Khorasan region (Iran’s North Eastern province), hosts an insect, which produces manna. Insects usually produce a gummy and sticky liquid, which is dried by the air and transformed into small, solid sticky particles. The manna sticks to the branches of *A. maurorum* [1–13].

When dry, it is fairly sweet yellowish resinous material resembling tear-shaped droplets measuring 1–3 mm. It has been widely used as a “herbal medicine.” However, its limited use as a food ingredient is likely due to low availability and lack of information. It has a significant

carbohydrate content, specifically sucrose (up to 42%). It is also a good source of iron (782 mg/kg), zinc (18.6 mg/kg), and copper (23.3 mg/kg) [3, 4].

Extensive research has been conducted on the medicinal properties of TM, uncovering a multitude of benefits. These include its antiprotozoal, antibiotic, antimicrobial, antibacterial, antifungal, antinociceptive, anti-inflammatory, antiulcer, diuretic, antidiarrheal, antiurolithiasis, antiacetylcholinesterase, NADH oxidase activity, and antioxidant properties. Based on the Medica manuscripts of Islamic Traditional Medicine, TM is prohibited in acute fever, smallpox, typhoid, bloody diarrhea, and hemorrhage. Traditionally, TM has been used in combination with other substances to treat various ailments. For example, its combination with butter relieves dysuria, with fresh milk enhances libido, and with cumin alleviates flatulence. A study on the total aqueous fraction of Tarangabin manna has revealed its potential immunostimulatory effects in the human body [1, 5, 6].

There are several publications focusing on the insect (*Poophilus nebulosus* Leth.) and its host (*A. maurorum*) and sparse research on the medicinal properties of TM, but no published article is available covering a thorough research on the techno-functional, rheological, and interfacial characteristics of Tarangabin manna (TM). An article by Farahnaky et al. [7] published limited data on physicochemical and rheological properties of Gaz-angabin, an exudate from *Astragalus adscendens* by *Cyamophila dicora*.

Therefore, this study aims to provide comprehensive data on the characteristics of TM suitable for its possible application in the food and pharmaceutical industries. Hence, various aspects of TM collected from the northern region of Iran were thoroughly tested and analyzed. For this purpose, physicochemical characteristics such as protein, fat, ash, moisture, sugar type and content, zeta potential, molecular weight, contact angle, structural (XRD, FTIR, and SEM), rheological (apparent viscosity, temperature-dependent viscosity, amplitude, and frequency sweep), emulsifying (interfacial and surface tension, and emulsion activity), and foaming properties (foaming ability and foaming stability) evaluated.

## 2. Material and Methods

**2.1. Material.** Tarangabin manna was collected from Kashmar, Khorasan Razavi, Iran. Canola oil was purchased from Narges Oil Company (Shiraz, Iran). Hexane, KBr, Toluene, and egg albumin were procured from Sigma-Aldrich (St. Louis, MO, USA).

**2.2. List of Abbreviations.** Fourier-transform infrared spectroscopy (FTIR), double-distilled water (DDW), X-ray diffraction (XRD), molecular weight (MW), zeta potential (ZP), contact angle (CA), interfacial tension (IFT), scanning electron microscopy (SEM), water activity (aw), activation energy (Ea), linear viscoelastic region (LVE), emulsifying index (EAI).

**2.3. Sample Purification.** TM crude powder (400 g) was dissolved in 500 mL double-distilled water (DDW) for 12 hours and filtered by a cloth filter to remove soil, thorns, and rocks. The filtrate was centrifuged at 5000 g for 10 min to eliminate remaining solid residue. The supernatant was then lyophilized, and purified TM powder was kept in polyethylene bags at 4°C. Purified TM (water-soluble component) is used at 0, 5, 25, and 50% (W/W) concentration for further analysis.

**2.4. Chemical Composition.** The moisture, protein (expressed as %  $N \times 5.75$ ), and ash content of the TM samples were determined according to the standard AOAC (2005) methods, specifically 925.1, 920.87, and 923.03, respectively. Each measurement was conducted in triplicate, and the reported values represent the average results [8].

**2.5. Sugar Analysis by HPLC.** Free sugar compositions were separately determined using the HPLC system (Knauer, Germany) equipped with Smartline pump 1000 and C18 column (Eurokat pb, particle size 10  $\mu$ m, length 300 mm, internal diameter 10 mm, Knauer, Germany) and RI detector 2300 at 65°C. TM (10000 ppm) was dissolved in DDW. The mobile phase comprised a DDW at a flow rate of 0.8 mL/min. The findings were determined by internal normalization of the chromatographic peak area. Ingredients were reported by comparing the relative retention times (RT) of peaks with standard sugars. The standards were fructose, mannitol, sucrose, glucose, xylose, mannose, and arabinose at the concentration of 0–1000  $\mu$ g/mL [9].

**2.6. Fourier-Transform Infrared Spectroscopy (FTIR).** The lyophilized TM powder was converted to the pellets after mixing with KBr with a ratio of 1:99. The FTIR spectrum was recorded by Thermo Nicolet Avatar 370 (Madison, WI, USA) and was inspected in the wavenumber ranged from 4000 to 400  $\text{cm}^{-1}$ .

**2.7. X-Ray Diffraction (XRD).** XRD pattern was performed by an X-ray powder diffractometer (Bruker AFX D8, Germany) at 40 kV and 40 mA. Data were reported from  $2\theta$  of 5° to 70°. This test was carried out on both the physically cleaned crude manna and freeze-dried purified powder.

**2.8. Molecular Weight (MW) Measurement.** The MW of lyophilized TM powder was measured by a dynamic light scattering instrument (DLS, SZ100, Horiba, Japan) working under the static mode at scattering angle of 90° at room temperature [10]. Various concentrations (ranging from 0.625 to 5 mg/mL) of samples were prepared in DDW.

**2.9. Zeta Potential (ZP).** ZP values of different TM solutions at concentrations of 1, 5, 25, and 50% were measured by the DLS technique (SZ100, Horiba, Japan) at room temperature using the Smoluchowski model. The samples were diluted with DDW in ratio of 1:100 before measurement [11].

### 2.10. Contact Angle (CA) and Interfacial Tension (IFT).

To measure the contact angle, thin layers of different TM solutions were applied onto glass slides and left to dry. A water droplet (2  $\mu\text{L}$ ) was then placed on the glass slide using a capillary tube. The contact angle of TM was determined using the static immobile drop method with a drop shape analyzer (DSA 100, KRÜSS GmbH, Hamburg, Germany). A CCD high-definition camera with a soft-focus lens was used to capture an image of the droplet. The analysis was performed using the software provided with the drop-shape analyzer [12].

To assess the oil-water interfacial tension (IFT) of purified TM, the pendant drop method was employed using the DSA 100 drop-shape analyzer. A drop of the TM solution was formed from a capillary tube immersed in pure canola oil. A photograph of the solution drop was captured using a high-speed CCD camera equipped with a macro lens. The interfacial tension was measured at the point where the drop detached from the needle, and the calculation was based on processing the shadow of the digital photo and utilizing the Laplace-Young equation [13].

**2.11. Scanning Electron Microscopy (SEM).** The surface morphology of the lyophilized TM powder was examined using a scanning electron microscope (SEM) (TESCAN Vega3, Czech Republic). The samples were affixed to an aluminum tape and coated with a thin layer of gold using a sputter coater (DSR1, Nanostructural Coating Co., Iran). Micrographs were captured at an accelerating voltage of 15 kV [14].

### 2.12. Rheological Properties

**2.12.1. Apparent Viscosity.** To assess the flow behavior of purified TM solutions (concentrations ranging from 1–50% w/v), measurements were conducted at 25°C using an Anton Paar MCR 302 rheometer (Graz, Austria). The rheometer was equipped with a cone-plate geometry (CP25-1) featuring a cone diameter of 25 mm, a gap size of 0.052 mm, and a cone angle of 1. To maintain a precise temperature control ( $\pm 0.1^\circ\text{C}$ ), a Peltier system was employed [15].

**2.12.2. Time Dependency.** The time-dependent flow behavior characteristics of different TM solutions (1 to 50% w/v) were studied at shear rate ( $\dot{\gamma}$ ) of  $100\text{ s}^{-1}$  over time (0 to 900 s).

**2.12.3. Temperature Dependency.** The apparent viscosity of purified TM solution at concentrations of 1, 5, 25, and 50% (w/v) was evaluated by heating the solutions from 20 to 60°C and cooling them from 60 to 20°C, at a constant shear rate of  $100\text{ s}^{-1}$ . This study was conducted following the guidelines provided in Section 2.12.1. Furthermore, the observed viscosity behavior was fitted to an Arrhenius model using MATLAB R2018b (MATLAB®, ver.9.5.0, 2018).

**2.12.4. Amplitude and Frequency Sweep Test.** To assess the rheological properties of purified TM solutions, dynamic measurements were conducted at room temperature. A CP25-1 cone-plate geometry on an Anton Paar rheometer was utilized for these tests. The solutions were prepared at concentrations of 1, 5, 25, and 50% (w/v). Amplitude sweep tests were conducted, subjecting the solutions to shear strains ranging from 0.01% to 100% at a constant frequency of 1 Hz. Furthermore, frequency sweep tests were performed within the linear viscoelastic (LVE) region, varying the frequency from 0.01 Hz to 100 Hz while maintaining a steady shear strain of 1%.

For each test, a carefully measured volume of 2 mL TM solution was placed on the rheometer plate and allowed to settle for 15 minutes. RheoCompass™ software was employed to analyze the rheological parameters, providing insights into the flow behavior of the solution, whether it displayed elastic or viscous characteristics [16].

**2.13. Surface Tension.** To determine the surface tension of purified TM solution, samples of various concentrations (1, 5, 25, and 50%) were dissolved slowly in DDW using a magnetic stirrer for 15 minutes at 300 rpm. Subsequently, the samples were left at room temperature for one day to complete the dehydration process and allow the surface tension to reach equilibrium.

To accurately measure the surface tension at room temperature, a digital tensiometer (Kino Industry, A201, USA) was employed. This instrument provided precise readings of the surface tension for each sample, ensuring accurate analysis. During the experiment, the platinum plate was immersed in the liquid, and the sensor detected the balance value in this submerged state. Subsequently, this value was converted into the corresponding surface tension value, which was then displayed for further examination.

**2.14. Emulsion Preparation and Characterization.** To evaluate the emulsifying ability, purified TM solutions at concentrations 1, 5, 25, and 50% (w/v) were hydrated in 17.50 mL of DDW. Subsequently, 7.5 g of pure canola oil was slowly added to each solution. The mixtures were homogenized using an Ultra-Turrax (T18, IKA, Germany) at 15,000 rpm for 2 minutes, following the method described by Naji-Tabasi and Razavi [17]. The emulsifying ability of each concentration of TM solution was determined using the approach outlined by Naji-Tabasi and Razavi [17]. Specifically, emulsions of each concentration of TM (100  $\mu\text{L}$ ) were freshly added to 25 mL of DDW, and the absorbance of the resulting emulsions was measured at 500 nm. This allowed for the assessment of the emulsification effectiveness of TM at different concentrations.

**2.15. Foam Preparation and Characterization.** The capability of purified TM to prepare egg albumin foam was determined using the model discussed by Naji-Tabasi and Razavi [17]. Briefly, egg albumin (0.3% w/v) was dissolved with 20 mL of

hydrated solution of TM at concentrations of 1, 5, 25, and 50% (w/v). Whipping was done intensely with speed of 15000 rpm by an Ultra-Turrax for 2 min. The amount of foam was calculated after production and then after 30 min. The ability of foaming and the stability of foaming were measured using the following equations:

$$\text{Ability of Foaming (\%)} = \left( \frac{V_{f0}}{V} \right) \times 100, \quad (1)$$

$$\text{Stability of Foaming (\%)} = \left( \frac{V_{f30}}{V_{f0}} \right) \times 100, \quad (2)$$

where  $V_{f0}$  is the volume of foam at the beginning,  $V_{f30}$  is the volume of the foam after 30 minutes, and  $V$  is the whole volume of solution.

**2.16. Statistical Analysis.** All experiments were conducted using a completely randomized design with three replications. The analysis of variances was performed, and Duncan's test (SAS® software, ver. 9.1, SAS Institute Inc., NC, USA) was employed to compare the means. A significance level of  $p < 0.05$  was used to evaluate significant differences between the means in the statistical analysis of quantitative data [18].

### 3. Results and Discussions

**3.1. Chemical Composition.** Results demonstrated that TM contains  $1.58\% \pm 0.23$  protein,  $2.98\% \pm 0.62$  moisture,  $0.51\% \pm 0.09$  fat,  $2.046\% \pm 0.06$  ash, and  $92.90\% \pm 0.53$  carbohydrate. The TM is a rich source of carbohydrate. Aynehchi [19] reported that Tarangabin had 26.44% sucrose, 11.64% fructose, 12.4% mucilage, and 5.8% ash. Sherahi et al. [20] reported that moisture content, protein, ash, fat, and carbohydrate of *Descurainia sophia* seed gum were 5.14, 2.12, 3.01, 0.77, and 78.23%, respectively. Ramezany et al. [2] reported that the ash and moisture content of Persian Manna were 3.5% and 4.57%, respectively. The protein content in this manna has an important role in the emulsifying activity and reducing interfacial tension [21].

**3.2. Sugar Analysis.** HPLC is a highly accurate and reliable method for analyzing manna exudates. Since sugars are not typically detectable using ultraviolet light, RI detectors are employed for their detection. Figure 1(a) displays the HPLC chromatogram obtained from the analysis of manna exudates.

In this study, the important carbohydrates found in the TM exudates, namely, mannitol (538.85 ppm) and sucrose (418.27 ppm), were quantified by generating a calibration curve. Additionally, xylose (16.36 ppm) was detected in the sample with the retention time of 16.67, 8.98, and 8.08, respectively. However, fructose, glucose, and arabinose were not detected using HPLC.

Previous research by Fakhri et al. [22] highlighted mannitol as the primary sugar present in manna exudates from certain cotoneaster species. Similarly, Caligiani et al.

[23] reported mannitol as the main sugar in manna exudates obtained from Sicilian *Fraxinus excelsior* L. Furthermore, Aynehchi [19] reported that Tarangabin contains 26.44% sucrose and 11.64% fructose. These findings provide valuable insights into the composition of TM and other manna exudates.

**3.3. FTIR Spectroscopy.** The purified TM powder underwent FTIR spectroscopy analysis to evaluate its functional groups and structural properties. Figure 1(b) displays the FTIR spectra of TM, and the corresponding peak assignments are provided in Table 1.

The broad absorption bands observed at  $3276 \text{ cm}^{-1}$  indicate the presence of various attributes, such as stretching bonds of free hydroxyl groups and O-H bands of carboxylic acid. Additionally, the absorption bands at  $2924 \text{ cm}^{-1}$  are assigned to stretching and bending vibrations of -CH<sub>2</sub>- and >CH- groups [24].

The absorption peaks at  $1412 \text{ cm}^{-1}$  and  $1627 \text{ cm}^{-1}$  indicate stretching vibrations of C=N and C=C bonds, respectively. Furthermore, the bands observed at  $1037 \text{ cm}^{-1}$  are attributed to stretching vibrations of C-O-C glycosidic bonds. The wide range of absorption between  $3500$  and  $3000 \text{ cm}^{-1}$  indicates the presence of functional groups like stretching bonds of free hydroxyl groups and O-H bands of carboxylic acid. The broad absorption bands at  $3000 \text{ cm}^{-1}$  and  $2800 \text{ cm}^{-1}$  are specified for stretching and bending vibrations of -CH<sub>2</sub>- and >CH- groups [25].

In the FTIR spectra, peaks observed in the range of  $800$ – $1200 \text{ cm}^{-1}$  correspond to C-O bands in carbohydrates, while peaks in the range of  $1300$ – $1500 \text{ cm}^{-1}$  are related to carboxyl groups of galacturonic acid, indicating the presence of sugars and carbohydrate structures in the manna. The peaks observed in the range of  $3200$ – $3400 \text{ cm}^{-1}$  are associated with hydrogen bonding involving hydroxyl groups. Additionally, peaks in the range of  $1600$ – $1700 \text{ cm}^{-1}$  correspond to the amide I group of proteins [25].

These findings obtained from the FTIR spectroscopy analysis provide valuable insights into the functional groups and structural properties of TM, shedding light on its composition and characteristics.

**3.4. X-Ray Diffraction.** XRD analysis is a valuable method for evaluating the crystalline and amorphous structure of carbohydrates. Each crystal structure exhibits a unique X-ray pattern. Figure 1(c) depicts the XRD curves of both the native and purified TM samples.

The results indicate that the structure of TM undergoes a transformation from crystalline to amorphous form after solution and drying. The purified TM sample exhibits a peak at  $20.95^\circ$ , which corresponds to the amorphous structure of carbohydrate samples. This amorphous structure is associated with higher solubility.

Previous research by Oetjen and Haseley [26] supports these findings, as they reported a significant increase in amorphous structure after freeze-drying a crystalline sample. Additionally, Rezaei et al. [27] reported that the solubility of almond gum is influenced by the crystalline

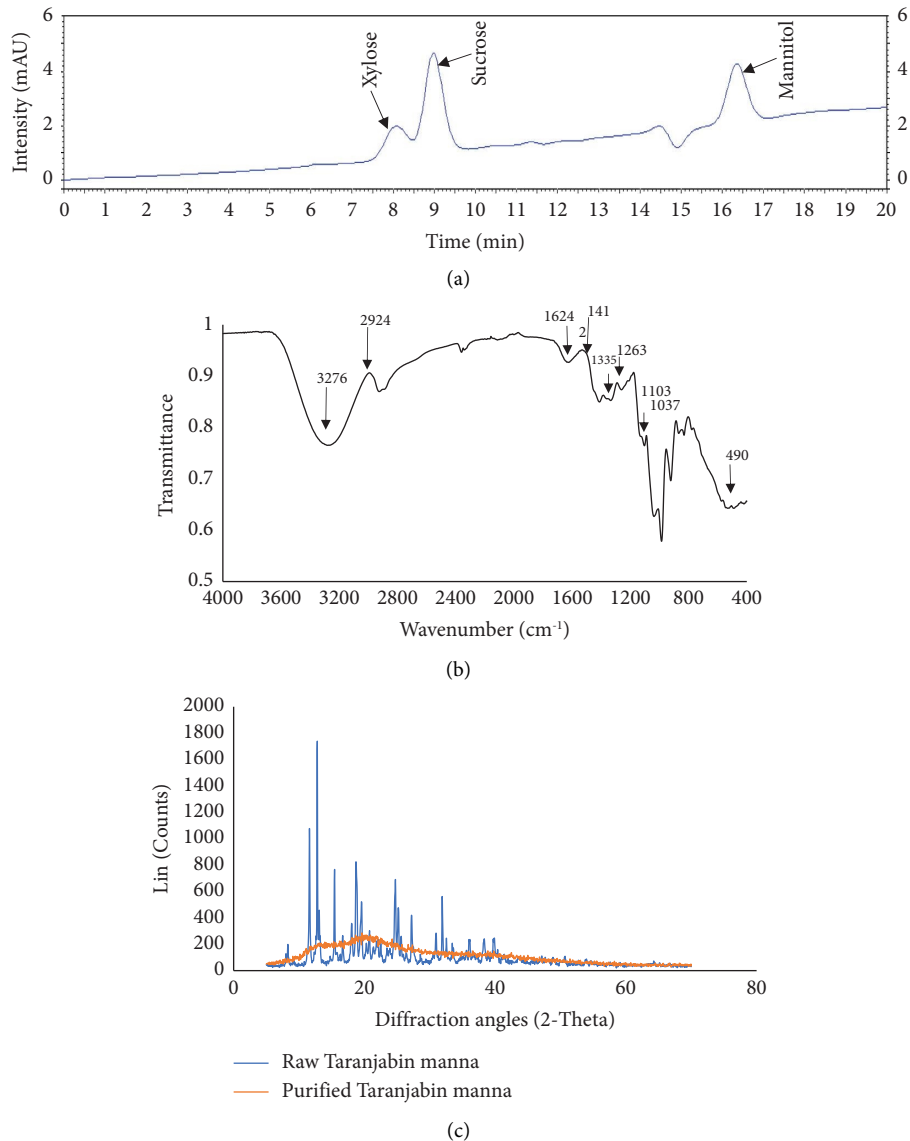


FIGURE 1: (a) HPLC characterization, (b) FTIR spectra, and (c) X-ray diffraction (XRD) patterns of the purified TM.

TABLE 1: FTIR peak assignments of purified Tarangabin manna.

Wave number (cm <sup>-1</sup> )	Assignment
3276.25	-OH stretching vibrations
2924.21	-CH <sub>2</sub> - and >CH- stretching and bending vibrations
1627.21	C=C stretching vibration and C=O stretching vibration
1412.59	C=N stretching vibration
1335.46	HCOO-
1263.03	-OH bending vibration
1103.52	C-N (aliphatic amine)
1037.42	C-O-C stretching vibrations of glycosidic bonds
490.23	C-C-O and C-O-C

structure of the gum. They found that the crystallinity index of the insoluble part, soluble part, and whole gum was 36.33%, 24.27%, and 26.46%, respectively. These observations from XRD analysis provide valuable insights into the

structural changes of TM, indicating a shift from crystalline to amorphous form during the purification process. The resulting amorphous structure contributes to its higher solubility.

**3.5. Molecular Weight (MW) and Zeta Potential.** The average molecular weight (MW) of TM was determined based on DLS method. The MW of TM was 7.8 kD, which was pretty low. MW of 1130 kD for *Commiphora africana* exudate [28], 5.17 and 16.4 kD for peach gums [29], and 0.24 and 2.95 kD for Acacia gums [30] were reported. Low rheological properties may be attributed to the low molecular weight of TM in comparison with other known carbohydrates and hydrocolloids. High molecular weight hydrocolloids having long chain usually show higher water absorption and viscosity [27].

The zeta potential of TM is exhibited in Figure 2(a). The results showed that zeta potential of 1, 5, 25, and 50% (w/v) of TM was  $-8.93$ ,  $-11.13$ ,  $-21.56$ , and  $-39.46$  mV, respectively. An almost 5-fold decrease in the zeta potential is observed as concentration increases by 50 times ( $p < 0.05$ ). The negative charge of TM is related to carboxyl and hydroxyl groups of TM, which detected in the FTIR spectra too. Zeta potential is an indication of the surface charge on the particle. Higher zeta potential is suitable for the production of stable colloidal systems, foaming, and emulsion system. By measuring the zeta potential of the solution, the amount of electrostatic repulsion forces between droplets of the same name (which prevents them from coming close to each other) can be determined [31].

**3.6. Contact Angle.** Contact angle was used for evaluating the material surface, hydrophobicity and hydrophilicity, and wettability of polymer surface. Contact angle measurement depends on various factors at macro- and microlevels. The contact angle of TM solution at various concentrations is demonstrated in Figure 2(b). The contact angle of 1, 5, 25, and 50% TM solutions after drying was 28.27, 28, 31.01, and 31.74°. There are not any significant differences between the samples ( $p > 0.05$ ). As shown in FTIR and zeta potential due to the presence of hydroxyl and carboxyl groups, the numerical value of contact angle shows that the TM had hydrophilic properties. Dupas et al. [32] evaluated the contact angle of sucrose at different particle sizes and maltodextrin at various molecular weights. They reported that the contact angle of sucrose is about to be  $15.8 \pm 0.3^\circ$  and maltodextrin varies between 30 and 3° depending on molecular weight.

**3.7. Scanning Electron Microscopy (SEM).** Figure 3 demonstrates SEM images of TM at 500 and 2000 magnifications. The results show that the sample had a unique and homogeneous surface without any porosity. Furthermore, the SEM photograms show that the size distribution of particles is mostly above 100  $\mu\text{m}$ , which may, to a great extent, influence the solubility of samples. Evaluating the surface of TM is important for future application. The higher specific surface of TM in the image is related to hydration and solubility of TM. This parameter had an effect on the viscosity and molecular weight of the sample [33, 34].

### 3.8. Rheological Properties

**3.8.1. Apparent Viscosity.** The results depicted in Figure 4(a) demonstrate that all TM solutions exhibit Newtonian behavior. This characteristic may be advantageous in the food

and pharmaceutical industries, particularly during pumping and filling processes, as Newtonian materials are less complicated to handle. Figure 4(a) illustrates the apparent viscosity of TM solutions at different concentrations. At a shear rate of  $30 \text{ s}^{-1}$  and a temperature of 25°C, the apparent viscosity of 1%, 5%, 25%, and 50% TM solutions was measured to be 1.1, 1.6, 2.4, and 12.4 MPa s, respectively.

These findings highlight the concentration-dependent viscosity of TM solutions, with higher concentrations exhibiting higher apparent viscosity values. This information is crucial for understanding the flow behavior of TM solutions and can aid in the design and optimization of processes in the food industry. Belay et al. [35] reported that Ethiopian monofloral honey had Newtonian behavior and their viscosity depends on moisture content, and they said that this could be because of the interaction of the ingredients with water, which reduce the honey liquid phase. So, the honey viscosity increased with decreasing the  $a_w$ . Kamboj et al. [36] also said four different Indian honey varieties had Newtonian behavior because of their sugar structure.

**3.8.2. Time Dependency.** When some fluids are exposed to a constant shear rate, they become thinner, thicker, or might be time-independent over time, which is related to changes in the inner structure. Time dependency of different concentrations of TM is presented in Figure 4(c). Various TM solutions revealed the time-independent behavior over time. Time dependency of sugar solution was related to the type of sugar, moisture content, and composition of ingredient and sugar concentration [37].

**3.8.3. Temperature Dependency.** Assessing the impact of heating on the viscosity of solutions is a crucial aspect in the food industry, as different solutions exhibit varying behaviors when subjected to temperature changes. Figure 4(d) illustrates the influence of temperature on the viscosity of TM solutions at different concentrations (1%, 5%, 25%, and 50% w/v). Notably, the solution with a concentration of 50% exhibited significantly higher viscosity compared to the other samples. As the TM solutions were heated to 60°C at a fixed shear rate, a reduction in viscosity was observed across all concentrations. This decrease in viscosity can be attributed to the breakdown of hydrogen bonding and weakening of intermolecular bonds within the TM molecules.

Understanding the changes in viscosity induced by heating is vital for optimizing food processes, as it allows for better control of the flow behavior and consistency of the solutions. Sun et al. [38] reported that the viscosity of polysaccharide solution decreased following a temperature increase. Lowering the solution temperature to 50°C reduces the viscosity to lower values indicating that the strength of biopolymer bonds for absorbing the water molecules surrounding themselves with the help of hydrogen bonds at lower temperatures. Similar results on the effects of heating on the viscosity were reported by Farhoosh and Riazi [39] and Gahruie et al. [10]. The reduction of viscosity during

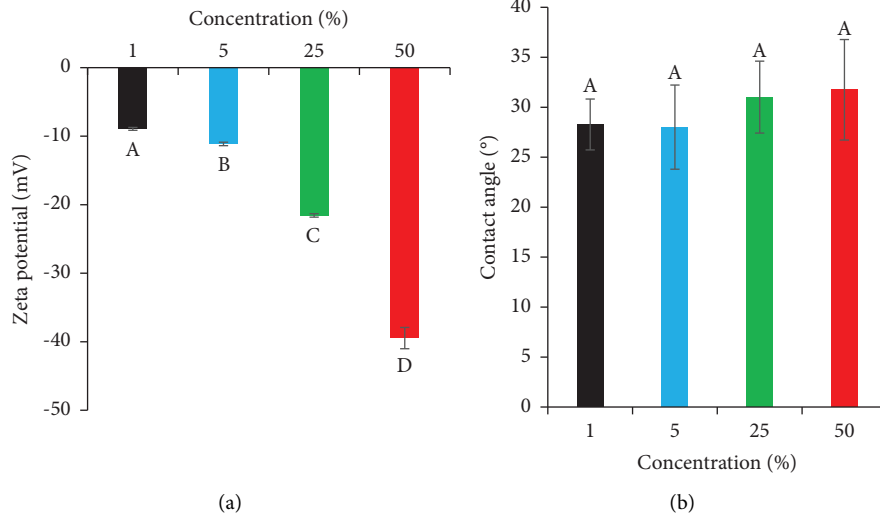


FIGURE 2: (a) Zeta potential and contact angle of different concentrations of TM and (b) contact angle of different concentrations of TM. The different capital letters indicate significant differences between samples at  $p < 0.05$ .

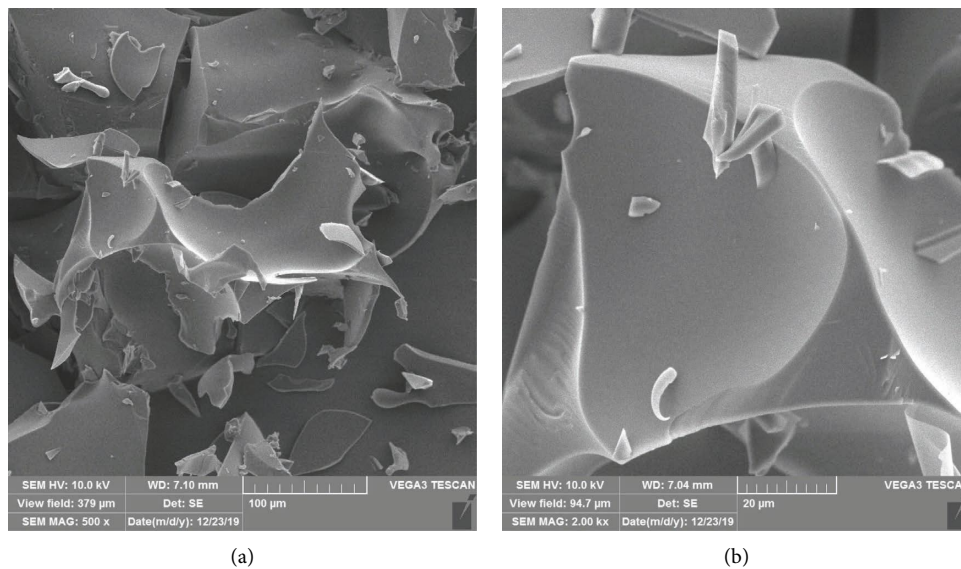


FIGURE 3: SEM micrograph of Tarangabin manna at different magnifications. (a) 500x and (b) 2000x.

heating is due to the mobility of molecules, the distance between molecules, and the weakening of interactions.

The temperature-viscosity relationship of TM solutions can be described by the Arrhenius model, as shown in Table 2. According to Eyring's theory, higher temperatures provide sufficient activation energy for the molecules to move more freely, resulting in increased fluid flow and filling of existing intermolecular spaces. The temperature dependency of hydrocolloid and sugar solutions can be well explained by the Arrhenius relation. Activation energy ( $E_a$ ) represents the energy required for the occurrence of primary flow processes and is influenced by various factors, such as polymer concentration, ionic strength, physicochemical properties of the polymer, and applied shear stress. In the case of TM solutions, the  $E_a$  values for 1% and 50%

concentrations were found to be the lowest (13493) and the highest (19514), respectively.

The effect of temperature on viscosity is closely linked to the structural properties of the solution, as reported by Sun et al. [38]. Considering the various structural properties of the purified manna, such as sugar type, ash content, carbon content, protein content, and molecular weight, different temperature sensitivities have been observed [40].

Understanding the temperature-viscosity behavior and its relationship with the structural properties of TM solutions is crucial for determining their application in different food processes. These findings provide insights into the factors influencing the temperature sensitivity of TM solutions and contribute to the optimization of their utilization in the food industry.

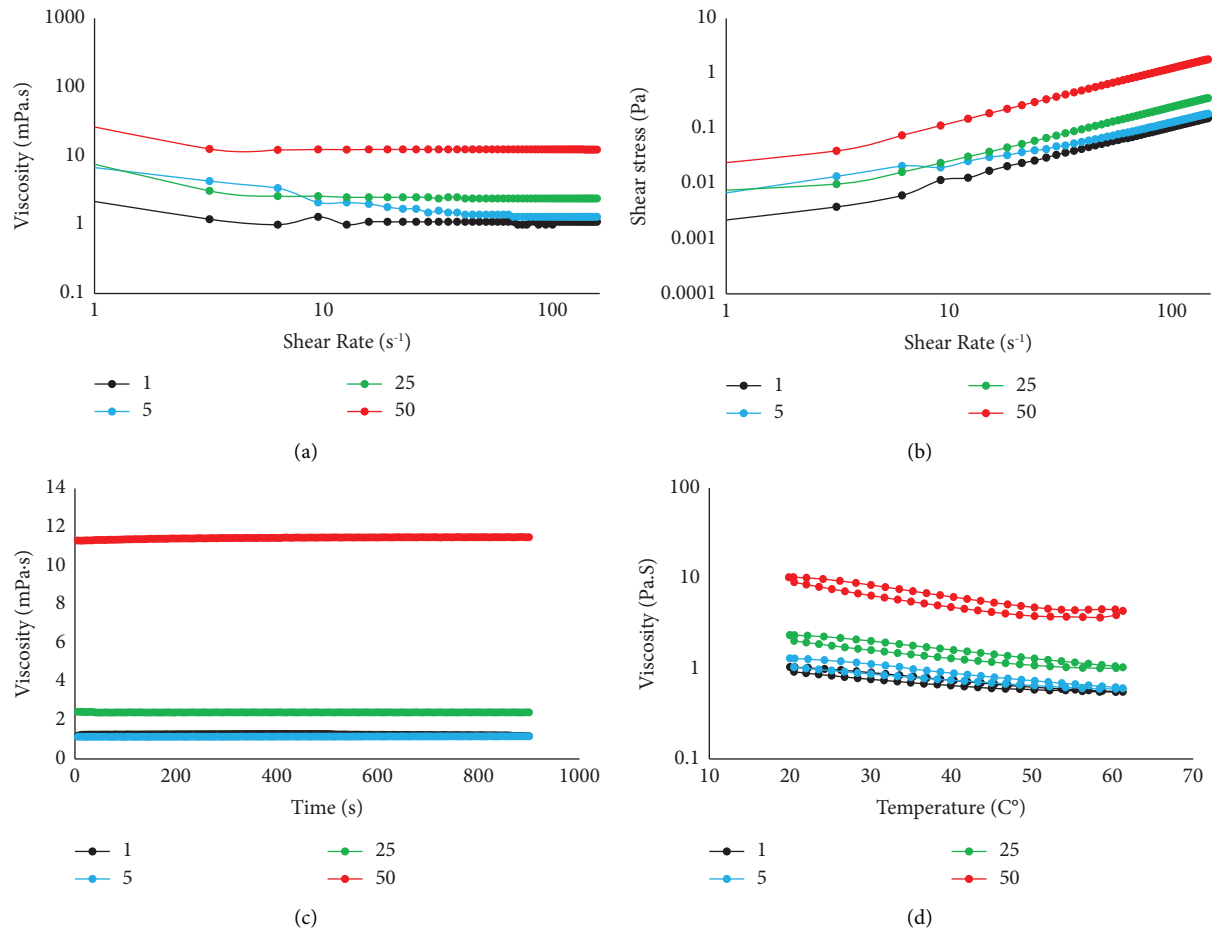


FIGURE 4: Effect of shear (a and b), time (c), and temperature (d) on the viscosity of different concentrations of TM. Also, 1, 5, 25, and 50 are the concentrations (%) of TM.

TABLE 2: Arrhenius model parameters of Tarangabin manna.

	Concentration (%)			
	1	5	25	50
Ea* (J/mol)	13493	15571	16384	19514
R <sup>2</sup>	99.44	99.31	99.17	98.48
RMSE	0.012	0.019	0.039	0.255

\*Ea: activation energy.

**3.8.4. Amplitude Sweep.** Dynamic rheological methods are commonly used to investigate the rheological properties of a wide range of hydrocolloid solutions, which exhibit viscoelastic behavior. These methods involve various procedures at both macroscopic and microscopic scales, contributing to a comprehensive understanding of the material's response [41].

In the case of TM solution, the strain sweep test results (Figure 5) indicated a liquid-like behavior, with the storage modulus ( $G'$ ) being lower than the loss modulus ( $G''$ ) within the linear viscoelastic region (LVE). The LVE region is crucial for distinguishing between strong and weak gels. Notably, the elastic and viscous characteristics of TM increased with higher concentrations, suggesting a more pronounced viscoelastic response.

**3.8.5. Frequency Sweep.** The frequency sweep test is a commonly used oscillation test in rheology. In this test, the amplitude of the input stress or strain remains constant, while the frequency is increased. Figures 5(a) and 5(b) illustrate the results of the frequency sweep test conducted at a fixed shear strain of 0.1% and frequencies ranging from 0.06 to 62.8 rad/s. Within this frequency range, all solutions exhibited a fluid-like behavior, as indicated by the storage modulus ( $G'$ ) being lower than the loss modulus ( $G''$ ) throughout the entire experimental range. The ratio of  $G''$  to  $G'$ , known as  $\tan \delta$  or the loss tangent, is shown in Figure 5(c). Typically, when  $\tan \delta$  is less than 1, the solution displays elastic characteristics, while values greater than 1 indicate a more viscous behavior. A  $\tan \delta$  higher than 0.1 suggests that the solution is not a true bulk gel [10].

Interestingly, the solution with a concentration of 50% exhibited a predominant elastic behavior or a weak gel-like composition across a wide range of applied frequencies, as depicted in Figure 5. In contrast, the other samples displayed liquid-like behavior.

Escriche et al. [42] reported that in eighteen honey samples,  $G''$  was higher than  $G'$ , indicating a more viscous viscoelastic behavior. They also noted that the rheological properties of honey are influenced by polymeric compounds



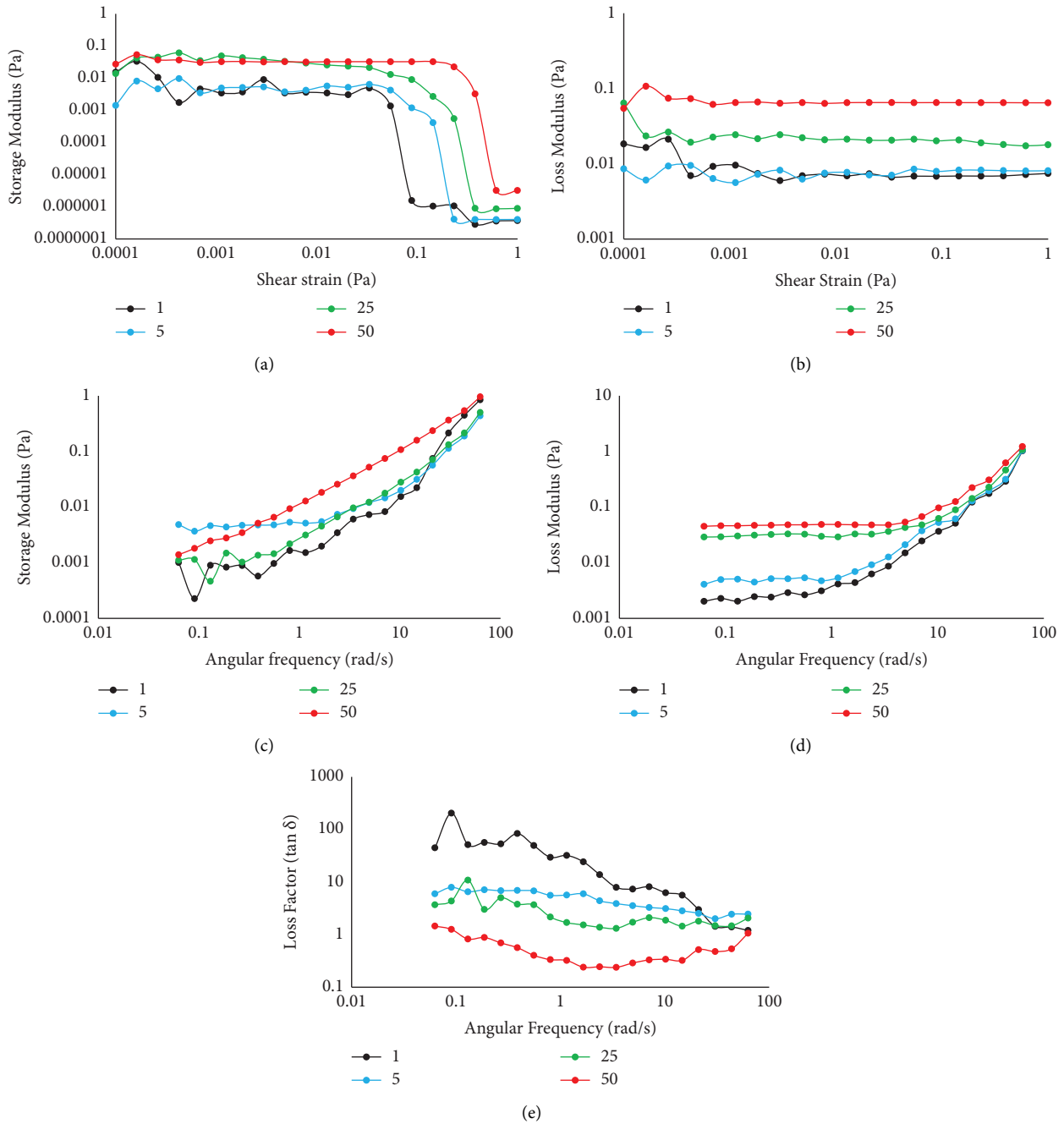


FIGURE 5: (a) Storage modulus ( $G'$ ) and (b) loss modulus  $G''$  of different concentrations of TM solution in amplitude sweep test, (c) storage modulus ( $G'$ ), (d) loss modulus ( $G''$ ), and (e) loss factor of different concentrations of TM solution in frequency sweep test.

and the structure of sugars, as glucose and fructose solutions exhibit different rheological properties.

These findings provide valuable insights into the frequency-dependent rheological behavior of the TM solutions, with the 50% concentration exhibiting a more gel-like composition, while the other samples displayed liquid-like behavior. The influence of polymeric compounds and the structure of sugars on the rheological properties are important factors to consider in understanding the behavior of these solutions.

**3.9. Interfacial Tension (IFT) and Surface Tension.** IFT among the water and oil was  $14.3 \pm 0.7$  mN/m in the absence of TM. A meaningful reduction in the interfacial tension (IFT) was observed after addition of TM ( $p < 0.05$ ). Reduction in IFT was influenced by TM solution concentration (Figure 6(a)). The IFT samples at 1, 5, 25, and 50% concentrations showed a reducing trend and were 14.29, 13.09, 9.67, and 7.74 mN/m, respectively. The surface activity of hydrocolloids is attributed to the existence of proteinaceous moiety, the polysaccharide complex, and its hydrophobicity [43]. A

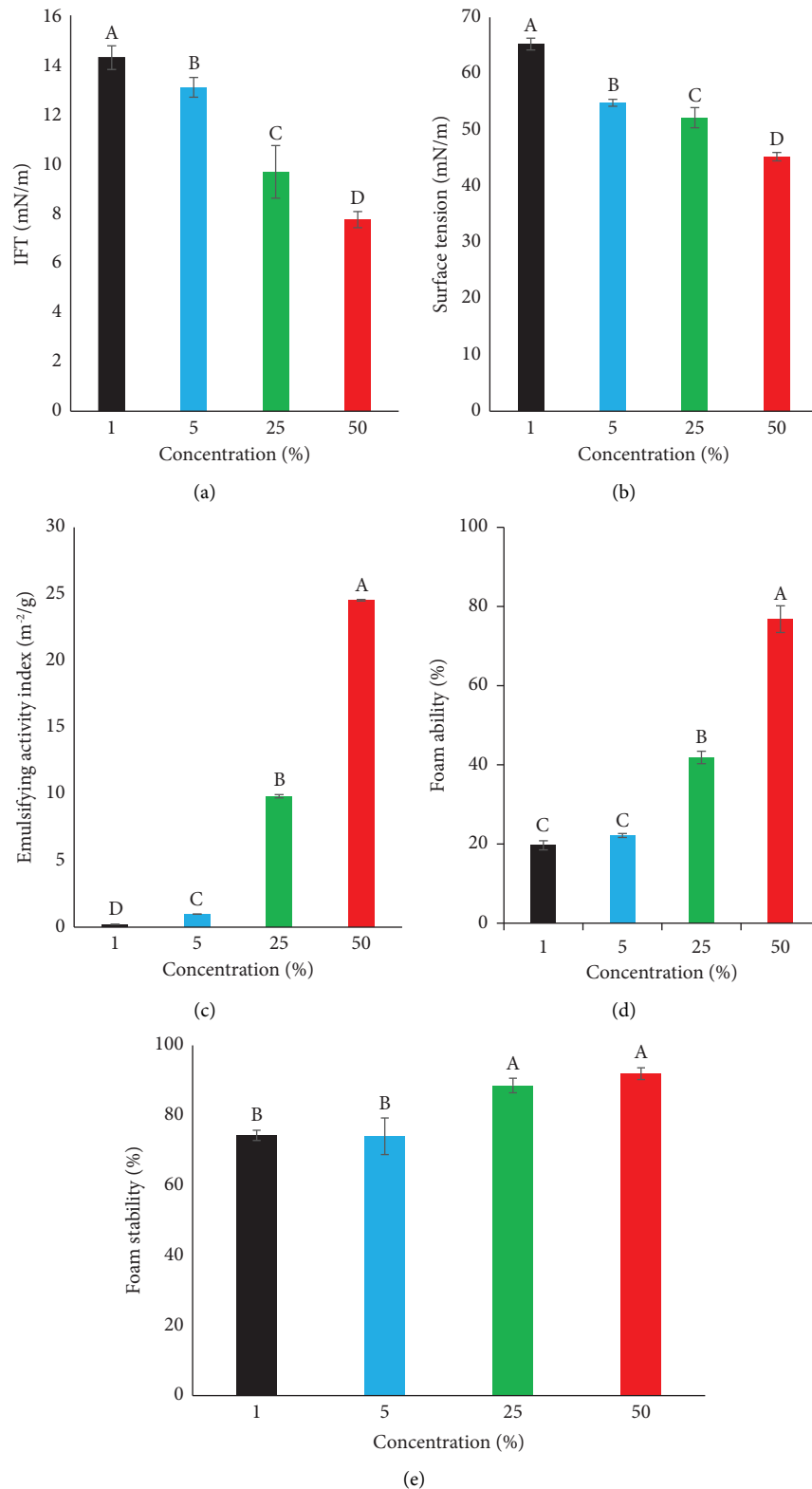


FIGURE 6: : IFT (a) and surface tension (b), emulsion activity (c), foaming ability (d), and foaming stability (e) of solution with varying concentrations of TM solution. The different capital letters indicate significant differences between samples at  $p < 0.05$ .

similar trend in the variation of IFT was observed in the surface activity of the purified powder. In the concentration range of 1 and 50%, the surface activity varies between 65

and 45 mN/m, respectively (Figure 6(b)). A similar trend was reported by Osano et al. [43] on variation of surface activities by type of hydrocolloids and their concentrations. The

surface tension of fenugreek, pectin, guar, xanthan, Arabic gum, and methyl cellulose at 0.5% concentration was 50.3, 53.6, 55.2, 60.8, 46.9, and 52.9 mN/m [44]. Furthermore, Koocheki et al. [45] reported that low molecular polysaccharides reduce the surface tension more than bigger polysaccharides.

**3.10. Emulsion and Foam Properties.** The emulsifying activity index (EAI) is a measure of the ability of external active factors, such as molecules and their arrangement, to create and stabilize emulsions. Figure 6(c) presents the emulsifying activity index of TM solutions at different concentrations.

Remarkably, the EAI values showed a significant increase as the concentration of TM solutions increased from 1 to 50% ( $p < 0.05$ ). This indicates that higher concentrations of TM solutions have a greater capability to form and stabilize emulsions. Understanding the emulsifying properties of TM solutions is essential in various applications, particularly in the food industry where emulsions play a crucial role in product formulation and stability. These findings highlight the concentration-dependent emulsifying activity of TM solutions and provide valuable insights for optimizing emulsion-based processes and product development. Hydrocolloids have the capability to enhance emulsion stability by increasing the viscosity of the continuous phase [10].

TM exhibited lower emulsifying activity index (EAI) compared to other hydrocolloids, such as basil seed gum (0.3%, 32 m<sup>2</sup>/g), asafoetida gum (1%, 38.6 m<sup>2</sup>/g), and Arabic gum (1%, 88 m<sup>2</sup>/g) [46].

The effects of TM concentration on foaming ability and foaming stability of albumin protein are shown in Figures 6(d) and 6(e). As the TM solution concentration increased from 1% to 50%, there was a notable increase in foaming ability, ranging from about 20% to 80%. No significant differences were observed between 1% and 5% samples, but the 50% sample exhibited significantly higher foam production ability compared to all other samples ( $p < 0.05$ ). Similarly, there were no significant differences in foaming stability between 1% and 5% samples, as well as between 25% and 50% samples.

Previous studies demonstrated that a 0.3% basil seed gum solution (containing 0.3% albumin) had a foaming ability of 28% [17]. The foaming stability and ability of different basil seed gums were associated with their surface activity and molecular weight. Hydrocolloids can enhance foam production capacity by reducing surface tension [17]. Foam ability refers to the capacity of a solution to sustain bubble size, foam mass, and liquid content over a period of time. Furthermore, the gas bubbles in foam ascend to the surface and eventually collapse [47]. Increasing the TM concentration resulted in increased foaming stability of albumin, which is influenced by the viscosity of the water phase.

## 4. Conclusion

The objective of this study was to comprehensively investigate the rheological, physicochemical, and interfacial properties of Tarangabin manna, an exudate obtained from

*A. maurorum*. Analysis revealed that TM contains more than 90% carbohydrates and less than 2% proteins. The presence of proteins in TM contributes to its remarkable emulsifying activity and the reduction of interfacial tension. Additionally, the exceptional solubility of TM can be attributed to its amorphous structure. The relatively low molecular weight of TM likely contributes to its Newtonian behavior and low viscosity. Notably, the TM solution at a concentration of 50% exhibited the lowest interfacial tension for the range of concentration analyzed. This finding suggests that the TM solution possesses excellent emulsifying and foam-forming abilities. These results collectively indicate that TM solution holds significant potential as a foaming and emulsifying agent in the food industry. Understanding the rheological, physicochemical, and interfacial properties of TM provides valuable insights into its potential applications and advantages in various food formulations. The exceptional emulsifying and foaming properties of TM make it an appealing choice for enhancing the texture and stability of food products.

## Data Availability

The data used to support the findings of this study are available from the corresponding author upon request.

## Conflicts of Interest

The authors declare that they have no known conflicts of interest.

## Authors' Contributions

All authors have significantly contributed to the development and the writing of this article.

## Acknowledgments

The authors would like to express sincere gratitude toward Shiraz University for their financial support of this MSc dissertation (M. Niakousari-Grant # 99GCB2M1981).

## References

- [1] S. Ansari, "Medicinal characteristics and therapeutic application of Manna/Taranjabeen (Alhagi pseudalhagi) in Unani medicine," *Annals of Ayurvedic Medicine*, vol. 8, no. 3, pp. 126–136, 2019.
- [2] F. Ramezany, N. Kiyani, and M. Khademizadeh, "Persian manna in the past and the present: an overview," *American Journal of Pharmacological Sciences*, vol. 1, no. 3, pp. 35–37, 2013.
- [3] R. A. Donkin, *Manna: An Historical Geography*, Springer, Berlin, Germany, 2013.
- [4] M. Mohammadi and M. Dini, "Identification of Manna Sources, production mechanism and utilization in Iran," *Iranian Journal of Medicinal and Aromatic Plants Research*, vol. 17, no. 1, pp. 75–109, 2003.
- [5] A. Parviz Tavassoli, M. Anushiravani, S. M. Hoseini et al., "Phytochemistry and therapeutic effects of Alhagi spp. and tarangabin in the Traditional and modern medicine:

- a review," *Journal of Herbmmed Pharmacology*, vol. 9, no. 2, pp. 86–104, 2020.
- [6] M. A. R. Salwa, A. A. E. Sawsan, F. D. Sahar, and A. K. Ashraf, "Antibacterial activity of some wild medicinal plants collected from western Mediterranean coast, Egypt: natural alternatives for infectious disease treatment," *African Journal of Biotechnology*, vol. 10, no. 52, pp. 10733–10743, 2011.
- [7] A. Farahnaky, Z. Shojaei, A. Sadeghi-Khomami, and M. Majzoobi, "Physicochemical properties and rheological behaviour of gaz-angubin," *International Journal of Food Properties*, vol. 12, no. 2, pp. 347–357, 2009.
- [8] P. Kaushik, K. Dowling, R. Adhikari, C. J. Barrow, and B. Adhikari, "Effect of extraction temperature on composition, structure and functional properties of flaxseed gum," *Food Chemistry*, vol. 215, pp. 333–340, 2017.
- [9] K. W. Se, R. K. R. Ibrahim, R. A. Wahab, and S. K. Ghoshal, "Accurate evaluation of sugar contents in stingless bee (*Heterotrigena itama*) honey using a swift scheme," *Journal of Food Composition and Analysis*, vol. 66, pp. 46–54, 2018.
- [10] H. H. Gahruie, M. H. Eskandari, M. Khalesi, P. Van der Meeren, and S. M. H. Hosseini, "Rheological and interfacial properties of basil seed gum modified with octenyl succinic anhydride," *Food Hydrocolloids*, vol. 101, Article ID 105489, 2020.
- [11] H. Gharanjig, K. Gharanjig, M. Hosseinnazhad, and S. M. Jafari, "Development and optimization of complex coacervates based on zedo gum, cress seed gum and gelatin," *International Journal of Biological Macromolecules*, vol. 148, pp. 31–40, 2020.
- [12] R. Malviya, S. Sundram, S. Fuloria et al., "Evaluation and characterization of tamarind gum polysaccharide: the biopolymer," *Polymers*, vol. 13, no. 18, p. 3023, 2021.
- [13] Y. Kazemzadeh, R. Parsaei, and M. Riazi, "Experimental study of asphaltene precipitation prediction during gas injection to oil reservoirs by interfacial tension measurement," *Colloids and Surfaces A: Physicochemical and Engineering Aspects*, vol. 466, pp. 138–146, 2015.
- [14] A. Golkar, J. M. Milani, A. Motamedzadegan, and R. E. Kenari, "Modification of corn starch by thermal-ultrasound treatment in presence of Arabic gum," *Scientific Reports*, vol. 12, no. 1, Article ID 19340, 2022.
- [15] S. M. H. Hosseini, H. Hashemi Gahruie, M. Razmjooie et al., "Effects of novel and conventional thermal treatments on the physicochemical properties of iron-loaded double emulsions," *Food Chemistry*, vol. 270, pp. 70–77, 2019.
- [16] J. Ahmed, "Effect of pressure, concentration and temperature on the oscillatory rheology of guar gum dispersions: response surface methodology approach," *Food Hydrocolloids*, vol. 113, Article ID 106554, 2021.
- [17] S. Naji-Tabasi and S. M. A. Razavi, "New studies on basil (*Ocimum basilicum* L.) seed gum: Part II—emulsifying and foaming characterization," *Carbohydrate Polymers*, vol. 149, pp. 140–150, 2016.
- [18] V. J. Kiprop, M. N. Omwamba, and S. M. Mahungu, "Influence of gum Arabic from *Acacia Senegal* var. *gt kerensis* on the modifications of pasting and textural properties of cassava and corn starches," *Food and Nutrition Sciences*, vol. 12, no. 11, pp. 1098–1115, 2021.
- [19] Y. Aynehchi, *Pharmacognosy and Medicinal Plants of Iran*, Tehran University, Tehran, Iran, 1986.
- [20] M. H. Sherahi, M. Fathi, F. Zhandari, S. M. B. Hashemi, and A. Rashidi, "Structural characterization and physicochemical properties of *Descurainia sophia* seed gum," *Food Hydrocolloids*, vol. 66, pp. 82–89, 2017.
- [21] Y. Brummer, W. Cui, and Q. Wang, "Extraction, purification and physicochemical characterization of fenugreek gum," *Food Hydrocolloids*, vol. 17, no. 3, pp. 229–236, 2003.
- [22] M. Fakhri, A. Davoodi, M. Parviz et al., "Characterization and HPLC analysis of manna from some cotoneaster species," *International Journal of Pharma Sciences and Research*, vol. 8, no. 12, pp. 5360–5366, 2017.
- [23] A. Caligiani, L. Tonelli, G. Palla, A. Marseglia, D. Rossi, and R. Bruni, "Looking beyond sugars: phytochemical profiling and standardization of manna exudates from Sicilian *Fraxinus excelsior* L.," *Fitoterapia*, vol. 90, pp. 65–72, 2013.
- [24] J. Kang, S. W. Cui, J. Chen, G. O. Phillips, Y. Wu, and Q. Wang, "New studies on gum ghatti (*Anogeissus latifolia*) part I. Fractionation, chemical and physical characterization of the gum," *Food Hydrocolloids*, vol. 25, no. 8, pp. 1984–1990, 2011.
- [25] R. Song, R. Wei, B. Zhang, Z. Yang, and D. Wang, "Antioxidant and antiproliferative activities of heated sterilized pepsin hydrolysate derived from half-fin anchovy (*Setipinna taty*)," *Marine Drugs*, vol. 9, no. 6, pp. 1142–1156, 2011.
- [26] G.-W. Oetjen and P. Haseley, *Freeze-drying*, John Wiley & Sons, Hoboken, NJ, USA, 2004.
- [27] A. Rezaei, A. Nasirpour, and H. Tavanai, "Fractionation and some physicochemical properties of almond gum (*Amygdalus communis* L.) exudates," *Food Hydrocolloids*, vol. 60, pp. 461–469, 2016.
- [28] A. Dahi, B. M.-L. Abdellahi, M. F. Deida, N. Hucher, C. Malhiac, and F. Renou, "Chemical and physicochemical characterizations of the water-soluble fraction of the *Commiphora africana* exudate," *Food Hydrocolloids*, vol. 86, pp. 2–10, 2019.
- [29] C. Wei, Y. Zhang, H. Zhang et al., "Physicochemical properties and conformations of water-soluble peach gums via different preparation methods," *Food Hydrocolloids*, vol. 95, pp. 571–579, 2019.
- [30] R. M. Daoub, A. H. Elmubarak, M. Misran, E. A. Hassan, and M. E. Osman, "Characterization and functional properties of some natural Acacia gums," *Journal of the Saudi Society of Agricultural Sciences*, vol. 17, no. 3, pp. 241–249, 2018.
- [31] V. Mohanta, G. Madras, and S. Patil, "Layer-by-layer assembled thin film of albumin nanoparticles for delivery of doxorubicin," *Journal of Physical Chemistry C*, vol. 116, no. 9, pp. 5333–5341, 2012.
- [32] J. Dupas, V. Girard, and L. Forné, "Reconstitution properties of sucrose and maltodextrins," *Langmuir*, vol. 33, no. 4, pp. 988–995, 2017.
- [33] G. L. de Pinto, M. Martinez, A. L. de Corredor, C. Rivas, and E. Ocando, "Chemical and <sup>13</sup>C NMR studies of *Enterolobium cyclocarpum* gum and its degradation products," *Phytochemistry*, vol. 37, no. 5, pp. 1311–1315, 1994.
- [34] F. Ohwoavworhwa and T. Adelakun, "Some physical characteristics of microcrystalline cellulose obtained from raw cotton of *Cochlospermum planchonii* Trop.," *Journal of Pharmacy Research*, vol. 4, no. 2, pp. 501–507, 2005.
- [35] A. Belay, G. D. Haki, M. Birringer et al., "Rheology and botanical origin of Ethiopian monofloral honey," *LWT- Food Science and Technology*, vol. 75, pp. 393–401, 2017.
- [36] R. Kamboj, G. A. Nayik, M. B. Bera, and V. Nanda, "Sugar profile and rheological behaviour of four different Indian honey varieties," *Journal of Food Science and Technology*, vol. 57, no. 8, pp. 2985–2993, 2020.
- [37] B. Mossel, B. Bhandari, B. D'Arcy, and N. J. L.-F. S. Caffin, "Use of an Arrhenius model to predict rheological behaviour

- in some Australian honeys,” *LWT- Food Science and Technology*, vol. 33, no. 8, pp. 545–552, 2000.
- [38] F. Sun, Q. Huang, and J. Wu, “Rheological behaviors of an exopolysaccharide from fermentation medium of a *Cordyceps sinensis* fungus (Cs-HK1),” *Carbohydrate Polymers*, vol. 114, pp. 506–513, 2014.
- [39] R. Farhoosh and A. Riazi, “A compositional study on two current types of salep in Iran and their rheological properties as a function of concentration and temperature,” *Food Hydrocolloids*, vol. 21, no. 4, pp. 660–666, 2007.
- [40] S. Razmkhah, S. M. A. Razavi, and M. A. Mohammadifar, “Purification of cress seed (*Lepidium sativum*) gum: a comprehensive rheological study,” *Food Hydrocolloids*, vol. 61, pp. 358–368, 2016.
- [41] A. P. Deshpande, “Oscillatory shear rheology for probing nonlinear viscoelasticity of complex fluids: large amplitude oscillatory shear,” *Rheology of Complex Fluids*, Springer, Berlin, Germany, 2010.
- [42] I. Escriche, M. Oroian, M. Visquert, M. L. Gras, and D. Vidal, “Rheological properties of honey from Burkina Faso: loss modulus and complex viscosity modeling,” *International Journal of Food Properties*, vol. 19, no. 11, pp. 2575–2586, 2016.
- [43] J. P. Osano, S. H. Hosseini-Parvar, L. Matia-Merino, and M. J. F. H. Golding, “Emulsifying properties of a novel polysaccharide extracted from basil seed (*Ocimum bacilicum* L.): effect of polysaccharide and protein content,” *Food Hydrocolloids*, vol. 37, pp. 40–48, 2014.
- [44] X. Huang, Y. Kakuda, and W. J. F. h. Cui, “Hydrocolloids in emulsions: particle size distribution and interfacial activity,” *Food Hydrocolloids*, vol. 15, no. 4-6, pp. 533–542, 2001.
- [45] A. Koocheki, S. M. Razavi, and M. A. J. F. B. Hesarinejad, “Effect of extraction procedures on functional properties of *Eruca sativa* Seed Mucilage,” *Food Biophysics*, vol. 7, no. 1, pp. 84–92, 2012.
- [46] S. Saeidy, A. Nasirpour, G. Djelveh et al., “Rheological and functional properties of asafoetida gum,” *International Journal of Biological Macromolecules*, vol. 118, pp. 1168–1173, 2018.
- [47] A. Govindu, R. Ahmed, S. Shah, and M. Amani, “Stability of foams in pipe and annulus,” *Journal of Petroleum Science and Engineering*, vol. 180, pp. 594–604, 2019.